JAERI-M
6867

EFFECT OF ELECTRON CHANNELING ON DAMAGE PRODUCTION IN A GERMANIUM CRYSTAL

January 1977

Takahiko NISHIDA and Kazuhiko IZUI

日本原子力研究所
Japan Atomic Energy Research Institute

JAERI-M 6867

Effect of Electron Channeling on Damage Production in a Germanium Crystal

Takahiko NISHIDA and Kazuhiko IZUI[+]

Division of Reactor Engineering, Tokai, JAERI

(Received December 14, 1976)

Three-dimensional, fine distributions of electron current density in a germanium crystal are calculated by the many-beam dynamical theory of electron diffraction for electrons incident parallel to the principal zone axes. It is found that two-dimensional distributions on the transverse plane oscillate along the depth direction and that a highly localized distribution around the rows of atoms and an almost flat distribution appear alternately with a definite period of depth. The effect of the localized current density on the damage production is discussed by introducing the effective current ratio J_{eff} which is defined as the ratio of the local current density at the rows of atoms to the mean current density for electrons incident parallel to the zone axis. The values of J_{eff} is higher in the order of the <100>, <111> and <110> directions. The energy dependence of J_{eff} in the <100> direction is also examined.

+ Division of Chemistry, Tokai, JAERI

JAERI－M 6867

ゲルマニウム結晶中の欠陥生成に対する電子チャンネリング効果

日本原子力研究所東海研究所
原子炉工学部

西田　雄彦・出井数彦*

（１９７６年１２月１４日受理）

ゲルマニウムの主な結晶軸方向に電子が入射した場合の電流密度の３次元詳細分布を，電子回折多波理論により計算した。この結果，入射方向に垂直な面上での２次元パターンは厚さと共に振動し，原子列近傍では，ある周期でピーク状と平担な分布が交互に現われることが分った。この２次元的に局在した電流密度の格子欠陥生成に及ぼす効果を，〝有効電流比〟，J_{eff} という量を導入して議論した。これはある結晶軸に沿って入射した電子により原子列のまわりに集中した電流密度と，単位セル内の平均電流密度の比として定義するが，入射方向については，＜１１０＞，＜１１１＞，＜１００＞ の順にこの比が増加する結果が得られた。又＜１００＞方向については，J_{eff}の入射エネルギー依存性も調べた。

* 日本原子力研究所東海研究所原子炉化学部

< CONTENT >

目　　次

1. Introduction

In the study of radiation damage due to high energy particle bombardment, it is of primary importance to know accurately the production rate of primary knock-ons. This quantity is given by a product of a displacement cross section and a current density of bombarding particles in a crystal. The displacement cross section is orientation-dependent in a crystalline material due to the anisotropy of the displacement threshold energy.[1] The current density of the injected particles has also an anisotropic property as is actually observed as channeling phenomena.[2] As for the localization of electrons, the intensity distributions of the individual Bloch waves associated with some of the branchs of the dispersion surface have been calculated in copper[3] and magnesium oxide crystals[4),5] by using the many-beam theory of electron diffraction. Recently, H. Hashimoto et al.[6] have calculated the density distribution of 1 and 3 Mev electrons in gold crystal taking into account the interference of whole excited Bloch waves and emphasized that the actual path of electrons can be evaluated by the current flow of total Bloch waves.

In the present paper we are concerned with the localization of the total current as a result of the interference of all Bloch waves. Using the current density formula, calculations are made along the axes of a germanium crystal by the many-beam theory of electron diffraction. Combining the classical picture of knock-on process with the localized current density, we present a model to estimate an "effective current density", J_{eff}, which is an important correction factor to the incident electron beam for estimating the electron flux effective for the atomic displacement in a crystal.

2. Method of Calculations

The total current density of electrons incident on the crystal in the <HKL> direction is expressed as

$$J^{T}_{<HKL>}(r) = \frac{\hbar}{2im}[\Psi^{*}(r)\mathrm{grad}\Psi(r) - \Psi(r)\mathrm{grad}\Psi^{*}(r)]$$

$$= \frac{2\pi\hbar}{m}\mathrm{Re}\Big[\sum_{j,j'} C_{o}^{(j')}C_{o}^{(j)*}\sum_{g,g'} C_{g}^{(j)}C_{g'}^{(j')*}(k_{o}^{(j)}+\beta_{g})e^{2\pi i\{k_{o}^{(j)}-k_{o}^{(j')}\cdot r+(g-g')r\}}\Big]$$

$$= J^{DT}_{<HKL>}(r) + J^{ODT}_{<HKL>}(r), \qquad [1]$$

1. Introduction

In the study of radiation damage due to high energy particle bombardment, it is of primary importance to know accurately the production rate of primary knock-ons. This quantity is given by a product of a displacement cross section and a current density of bombarding particles in a crystal. The displacement cross section is orientation-dependent in a crystalline material due to the anisotropy of the displacement threshold energy.[1] The current density of the injected particles has also an anisotropic property as is actually observed as channeling phenomena.[2] As for the localization of electrons, the intensity distributions of the individual Bloch waves associated with some of the branchs of the dispersion surface have been calculated in copper[3] and magnesium oxide crystals[4),5] by using the many-beam theory of electron diffraction. Recently, H. Hashimoto et al.[6] have calculated the density distribution of 1 and 3 Mev electrons in gold crystal taking into account the interference of whole excited Bloch waves and emphasized that the actual path of electrons can be evaluated by the current flow of total Bloch waves.

In the present paper we are concerned with the localization of the total current as a result of the interference of all Bloch waves. Using the current density formula, calculations are made along the axes of a germanium crystal by the many-beam theory of electron diffraction. Combining the classical picture of knock-on process with the localized current density, we present a model to estimate an "effective current density", J_{eff}, which is an important correction factor to the incident electron beam for estimating the electron flux effective for the atomic displacement in a crystal.

2. Method of Calculations

The total current density of electrons incident on the crystal in the <HKL> direction is expressed as

$$J^{T}_{<HKL>}(r) = \frac{\hbar}{2im}[\Psi^{*}(r)\,\mathrm{grad}\Psi(r) - \Psi(r)\,\mathrm{grad}\Psi^{*}(r)]$$

$$= \frac{2\pi\hbar}{m}\mathrm{Re}\Big[\sum_{j,j'} C_{o}^{(j')}C_{o}^{(j)*}\sum_{g,g'} C_{g}^{(j)}C_{g'}^{(j')*}(k_{o}^{(j)}+\beta_{g})\,e^{2\pi i\{k_{o}^{(j)}-k_{o}^{(j')}\cdot r+(g-g')r\}}\Big]$$

$$= J^{DT}_{<HKL>}(r) + J^{ODT}_{<HKL>}(r), \qquad [1]$$

here $\beta_g = \frac{1}{a}(h\Theta_x + k\Theta_y + \ell\Theta_z)$,

$$J^{DT}_{<HKL>}(r) = \frac{2\pi\hbar}{m}\mathrm{Re}\left[\sum_j |C^{(j)}_o|^2 \sum_{g,g'} C^{(j)}_g C^{(j)*}_{g'} (k^{(j)}_o + \beta_g) e^{2\pi i(g-g')r}\right], \quad [2]$$

$$J^{ODT}_{<HKL>}(r) = J_{<HKL>}(r) - J^{DT}_{<HKL>}(r),$$

$$\Psi(r) = \sum_j C^{(j)*}_o \sum_g C^{(j)}_g \, e^{2\pi i(k^{(j)}_o + g)\cdot r}, \quad [3]$$

where a is the lattice constant, and Θ_x, Θ_y and Θ_z are directional cosines of the normal of (HKL) plane to each of the cube edges of a unit cell, respectively. Reciprocal lattice vectors g (hkl) lie on the plane perpendicular to the <HKL> direction. The transmitted wave vector $k^{(j)}_o$ and the exicitation amplitude $C^{(j)}_o$ of Bloch wave $\Psi(r)^{(j)}$ are obtained from eigenvalues and eigenfunctions of an eigenvalue problem derived from the many-beam dynamical theory. The coordinate system for r (u_1, u_2, u_3) is illustrated in Fig. 1 (a).

From a simple calculation it is shown that

$$J^{DT}_{<HKL>}(u_1,u_2) = \overline{J^{T}_{<HKL>}(u_1,u_2)}, \text{ (average } u_3). \quad [4]$$

That is, $J^{DT}_{<HKL>}(u_1,u_2)$ which we call "diagonal total current density" is equal to the depth average of the total current density $J^{T}_{<HKL>}(u_1,u_2,u_3)$.

The damage production due to high energy electron bombardment is a result of highly localized interaction between incident electrons and lattice atoms. A knock-on occurs, in the classical picture, only when the electron with an energy of the order of 1 MeV approaches within the distance of the order of 10^{-4} Å from the atomic nucleus.

Here we introduce a concept of an "effective current ratio", J_{eff} which is defined as the ratio of the local current density effective for atomic displacement within the narrow cylindrical region S around the rows of the atomic nuclei to the mean current density. The J_{eff} can be expressed, using $J^{DT}_{<HKL>}(u_1,u_2)$ as follows,

$$J_{eff,<HKL>} = \frac{\frac{1}{s}\iint_s J^{DT}_{<HKL>}(u_1,u_2)\,du_1du_2}{\overline{J^{DT}_{<HKL>}(u_1,u_2)}}, \quad [5]$$

where the denominator is the average over the area of one periodic unit in the u_1 - u_2 plane.

The main quantities calculated in the present work are the profiles of J^T $(0,0,u_3)$ along the <100> direction of incidence, two-dimensional distributions of both J^T (u_1,u_2,u_3) and J^{DT} (u_1,u_2) displayed as contour-maps in the transverse planes perpendicular to the incident directions of some principal zone axes and finally J_{eff} for the <100>, <110> and <111> axial cases. Screens on which the contour-maps of the current densities are drawn are illustrated in Fig. 1 (b).

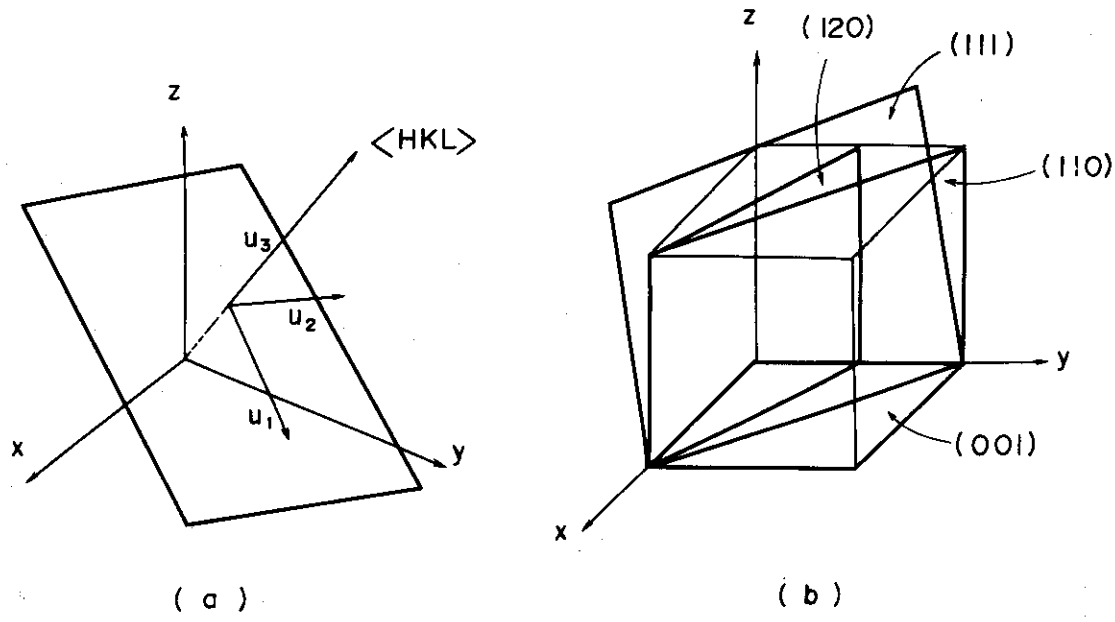

Fig. 1 Coordinate systems and the screens in the calculation. (a) x, y, z axes are taken to coincide with the cube edges of the unit cell of Ge. u_1 and u_2 axes lie on the (HKL) plane and u_3 axis is normal to the (HKL) plane. (b) Screens on which the contour-maps of the current density distributions are drawn for the <100>, <110>, <111> and <120> directions of incidence, respectively.

The computations were carried out by modifying the Program System MSCOPE-I[7] which was developed for FACOM-230-60 computer in JAERI. The effect of the number of beams used in the calculation is examined in some cases as will be described in Sec. 3. For most cases 61-beams were used except for the contour-maps of J^T (u_1,u_2,u_3) and J^{DT} (u_1,u_2), which were obtained by 13-beams or so. As for the atomic scattering factors, use was made of the Smith and Burge's analytical expressions.[8] The effect of electron absorption was not taken into account in the present work. The

energy of an incident electron is taken to be 1 MeV in this computation except for the cases examining the energy dependence of J^{DT} and J_{eff}.

3. Results of Calculations and Discussions

3.1 Three-dimensional distributions of the total current density

As expected from eq. [1], the total current density $J^T_{<HKL>}$ oscillates in the <HKL> direction with a period determined from eigenvalues $|k_o^{(j)}|$ (j=1,2,···n). For the electrons incident parallel to the <100> axis, the results of 13-and 61-beam calculations of $J_{<100>}$ are shown in Fig. 2. These two curves clearly show simple oscillations like a sine square curve. The period of the oscillation decreases with increasing the number of beams used in the calculations, as is seen in this figure. For the incidence of the off-axis direction ($k_{//} = -g_{2\bar{2}0}$, where $k_{//}$ is the component of k_o on the $u_1 - u_2$ plane), it is also shown in Fig. 2 that the depth oscillation of the total current density is rather irregular.

The same tendency is realized also for other incident directions, <110> and <111>. Such behaviors can be easily understood from a comparison among the values of the excitation amplitude, $C_o^{(j)}$ for these cases mentioned above. That is, for the axial case, there are only a few main terms of $C_o^{(j')*} \cdot C_o^{(j)}$ (j'=j) as shown in Table 1, which actually determine the simple mode of the depth-oscillations, while, for the off-axis case, many terms of $C_o^{(j')*} \cdot C_o^{(j)}$ of the comparable order compete with one another and result in the irregular mode of the depth oscillation. The distribution of the total current density in the transverse plane is also important, as it gives a clear image of the localization of electrons around the atomic rows. This two-dimensional distribution in the transverse plane is found also to oscillate with depth. This aspect is shown in Fig. 3, which is the results of 13-beam calculations of $J^T_{<100>}$ for the <100> axial case. The contour-maps in the upper part of Fig. 3 show the distributions of $J^T_{<100>}$ in the $u_1 - u_2$ planes at the depths of u_3 = 50 Å, 125 Å and 250 Å, respectively. The curves shown in the lower part of Fig. 3 are the profiles of $J^T_{<100>}$ along u_1 at $u_2 = 0$. These values of the depth correspond to the positions at which $J^T_{<100>}(0,0,u_3)$'s show almost minimum, maximum and middle values, respectively (see Fig. 2). From further computations it is confirmed that these patterns repeat with the definite periods of the depth, 280 Å for 13-beam and 190 Å for 61-beam computation. This sharp localization of electrons around the atomic rows appears and disappears period-

energy of an incident electron is taken to be 1 MeV in this computation except for the cases examining the energy dependence of J^{DT} and J_{eff}.

3. Results of Calculations and Discussions

3.1 Three-dimensional distributions of the total current density

As expected from eq. [1], the total current density $J^{T}_{<HKL>}$ oscillates in the <HKL> direction with a period determined from eigenvalues $|k_o^{(j)}|$ (j=1,2,$\cdots$n). For the electrons incident parallel to the <100> axis, the results of 13-and 61-beam calculations of $J_{<100>}$ are shown in Fig. 2. These two curves clearly show simple oscillations like a sine square curve. The period of the oscillation decreases with increasing the number of beams used in the calculations, as is seen in this figure. For the incidence of the off-axis direction ($k_{//} = -g_{2\bar{2}0}$, where $k_{//}$ is the component of k_o on the $u_1 - u_2$ plane), it is also shown in Fig. 2 that the depth oscillation of the total current density is rather irregular.

The same tendency is realized also for other incident directions, <110> and <111>. Such behaviors can be easily understood from a comparison among the values of the excitation amplitude, $C_o^{(j)}$ for these cases mentioned above. That is, for the axial case, there are only a few main terms of $C_o^{(j')*} \cdot C_o^{(j)}$ (j'=j) as shown in Table 1, which actually determine the simple mode of the depth-oscillations, while, for the off-axis case, many terms of $C_o^{(j')*} \cdot C_o^{(j)}$ of the comparable order compete with one another and result in the irregular mode of the depth oscillation. The distribution of the total current density in the transverse plane is also important, as it gives a clear image of the localization of electrons around the atomic rows. This two-dimensional distribution in the transverse plane is found also to oscillate with depth. This aspect is shown in Fig. 3, which is the results of 13-beam calculations of $J^{T}_{<100>}$ for the <100> axial case. The contour-maps in the upper part of Fig. 3 show the distributions of $J^{T}_{<100>}$ in the $u_1 - u_2$ planes at the depths of u_3 = 50 Å, 125 Å and 250 Å, respectively. The curves shown in the lower part of Fig. 3 are the profiles of $J^{T}_{<100>}$ along u_1 at $u_2 = 0$. These values of the depth correspond to the positions at which $J^{T}_{<100>}(0,0,u_3)$'s show almost minimum, maximum and middle values, respectively (see Fig. 2). From further computations it is confirmed that these patterns repeat with the definite periods of the depth, 280 Å for 13-beam and 190 Å for 61-beam computation. This sharp localization of electrons around the atomic rows appears and disappears period-

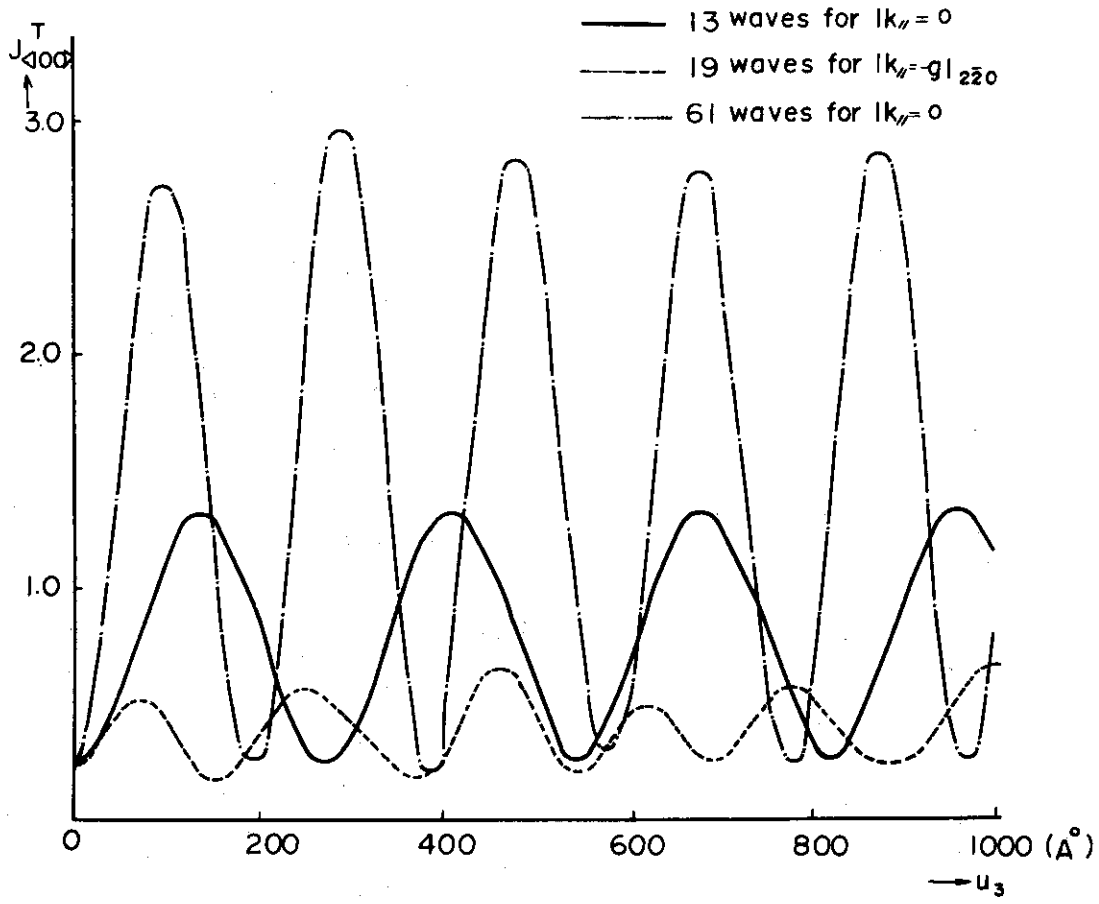

Fig. 2 Depth oscillations of the total current density, $J^T_{<100>}$. The solid and dash-dotted curves are obtained by 13-and 61-beam calculations, respectively. The dotted curve is obtained by 19-beam calculation for the slightly off-axis direction from the <100> axis ($k_{//} = - g_{2\bar{2}0}$).

Table 1 Dominant values of excitation amplitudes $C_o^{(j)}$ in some axial and off-axial cases.

Direction	Number of beam	Dominant values of $\lvert C_o^{(j)} \rvert_{(0.1 \leqq \lvert C_o^{(j)} \rvert \leqq 1)}$
<100>	13	$0.517^{(1)}$, $0.556^{(2)}$, $0.646^{(4)}$
<110>	17	$0.483^{(1)}$, $0.192^{(9)}$, $0.833^{(5)}$, $0.189^{(6)}$
<111>	13	$0.853^{(4)}$, $0.521^{(1)}$
<120>	15	$0.962^{(1)}$, $0.271^{(2)}$
<100> off axis	19	$0.327^{(1)}$, $0.412^{(2)}$, $0.440^{(4)}$, $0.178^{(3)}$, $0.497^{(5)}$, $0.263^{(6)}$, $0.274^{(7)}$, $0.227^{(9)}$, $0.188^{(8)}$

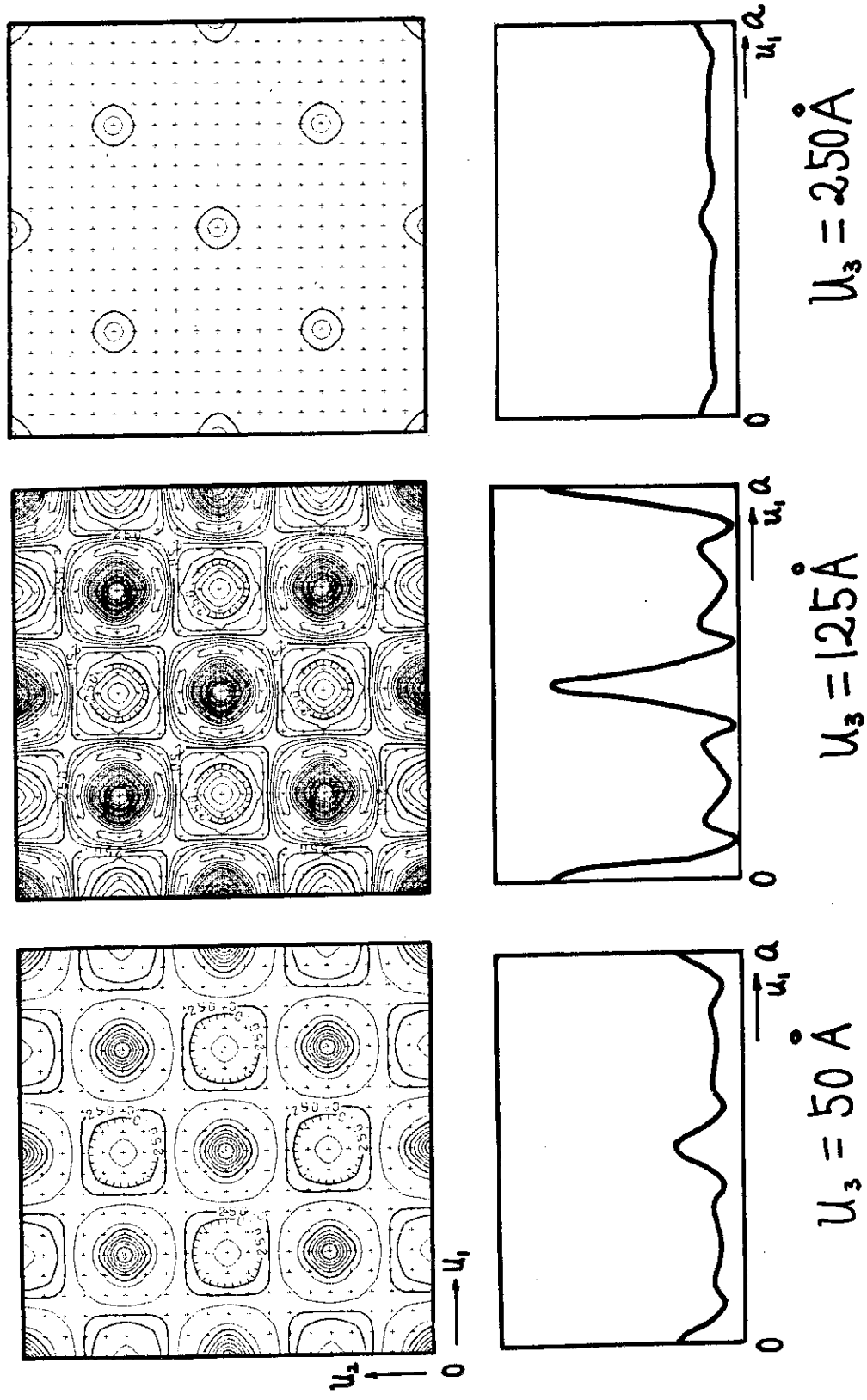

Fig. 3 Distributions of the total current density in the transverse plane at the depths of 50 Å, 125 Å and 250 Å for the <100> direction of incidence. The curves in the lower part are the profiles along u_1 at $u_2 = 0$.

ically with the depth, and the total current density integrated over the area of the periodic unit of the lattice in the transverse plane is conserved at all depths. The period of this depth oscillation is quite interesting in contrast to the ordinary extinction distance associated with each of the transmitted and diffracted beams, and may be called as "localization period of electron current".

3.2 Dependence of incident directions on $J^{DT}_{<HKL>}$

Here we are concerned with the diagonal total current density, J^{DT} which is equal to the depth average of the total current density as described in Sec. 2. Figures 4(a)∿(d) show the contour-maps of J^{DT} on the transverse planes perpendicular to the <100>, <110>, <111> and <120> directions of incidence, respectively. In the lower part of these figures, positions of atomic rows on each screen (see Fig. 1 (b)) are schematically shown together with the profiles of J^{DT} along u_1 at $u_2 = 0$ in the middle part. The positions of a highest peak in the contour-maps coincide with the positions of the atomic rows, revealing the strong concentration of electrons in the vicinity of the atomic rows. The peak height is differed depending on the incident directions. There exist also some subpeaks or somma-like shapes between the atomic rows as shown in the contour-maps. The characteristic feature seen in the <111> axial case is that the current density in the interspace among the atomic rows is predominantly larger than those in the other cases. This would be interesting in connection with the problem of electron absorption. For the <120> axial case, there exists a strong localization of electrons at the atomic planes parallel to the (001) plane, exhibiting the aspect of plannar channeling. Figure 5 shows the contour-maps of the diagonal total current density and some of the constitutional current densities in each wave field associated with each branch of the dispersion surface for the <110> axial case. The wave field 1 reveals a strong concentration of electrons in the vicinity of the atomic rows, while the others show localized distributions between the atomic rows in respective characteristic ways as is seen in Fig. 5.

3.3 Directional dependence of the effective current ratio J_{eff}

The main purpose of the present paper is the estimation of the "effective current ratio" which is described in Sec. 2 as a measure of localized current density around the atomic nuclei, which is effective for

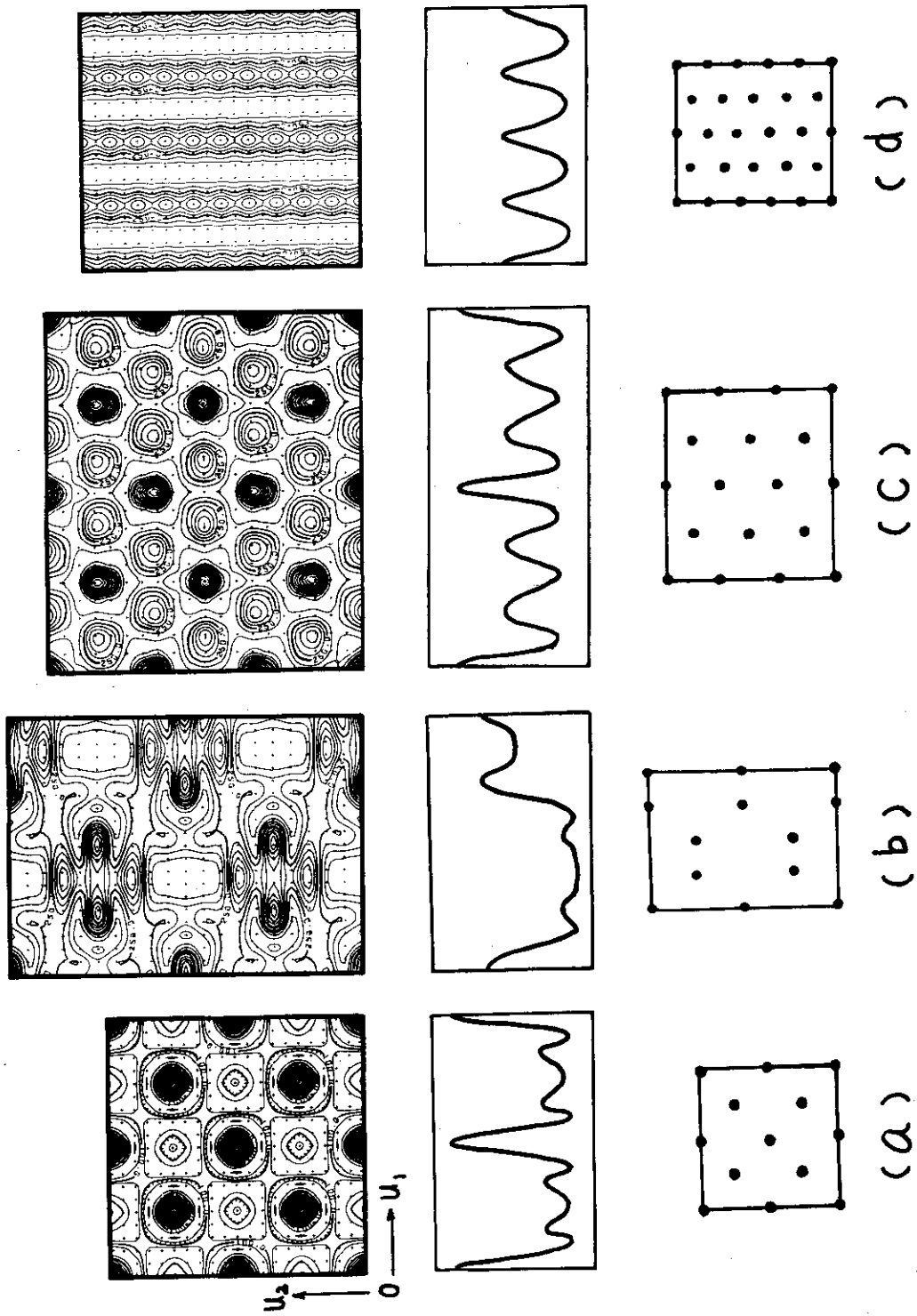

Fig. 4 The directional dependence of the two-dimensional distributions and the profiles of diagonal total current density in the transverse plane, and the projected positions of atoms on the transverse planes in (a), (b), (c) and (d) for the <100>, <110>, <111> and <120> directions of incidence, respectively.

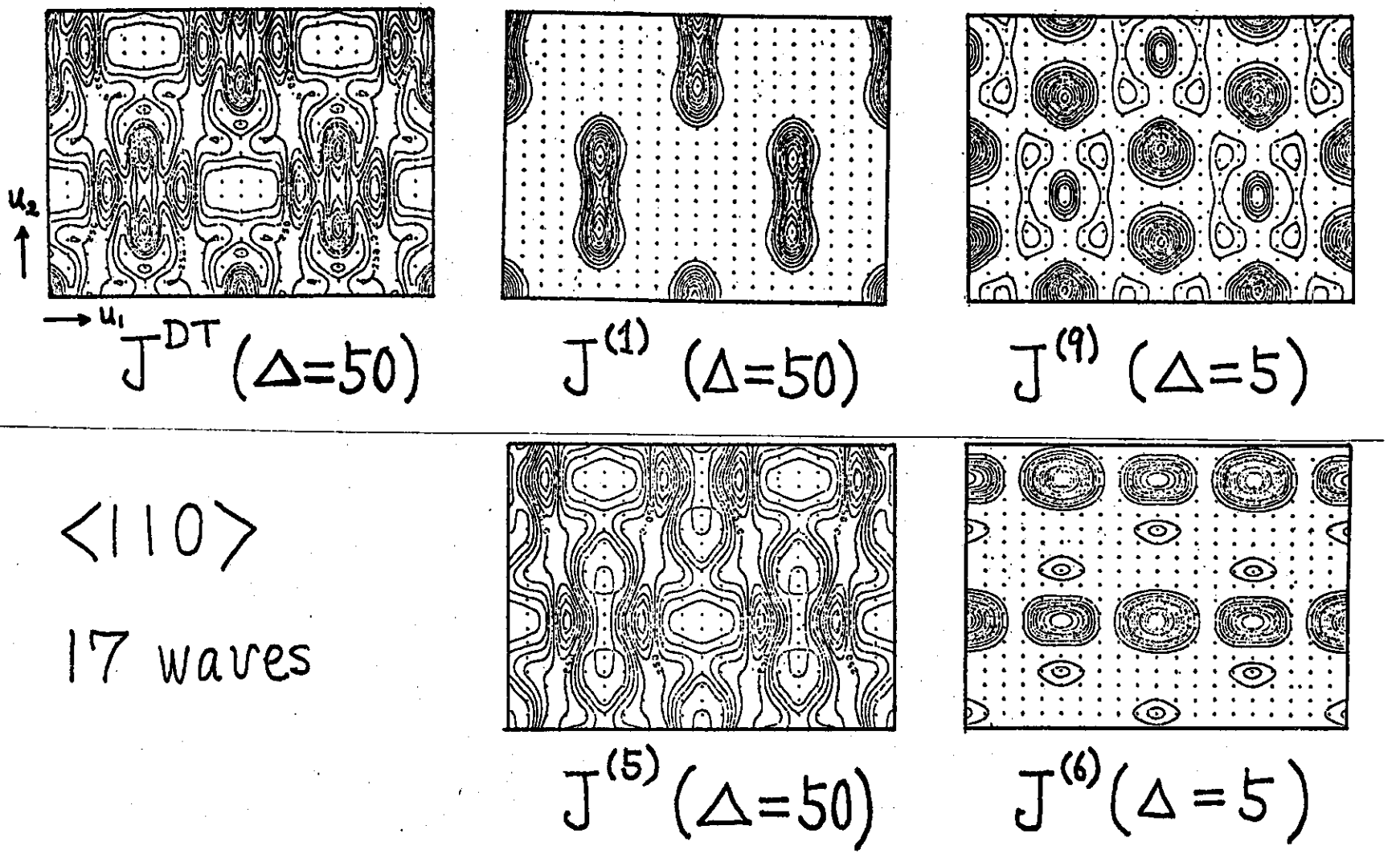

Fig. 5 Contour-maps of diagonal total current density J^{DT} and its components $J^{(1)}$, $J^{(5)}$, $J^{(6)}$ and $J^{(9)}$ obtained by 17-beam calculation for the <110> axial case. The j of $J^{(j)}$ indicates the number of the branches of the dispersion surface and Δ the width of contour-lines.

JAERI-M 6867

atomic displacements. At first we have checked the effect of the number of beams used in the calculations on the profile of the diagonal total current density around the atomic nuclei. The result is shown in Fig. 6, where 13-, 61-and 85-beam are used for 1 MeV electrons incident parallel to the <100> axis and the atomic nuclei is placed at $u_1 = u_2 = 0$. It is seen in this figure that the discrepancy between the results of 61-and 85-beam calculations is rather small, whereas the result of 13-beam calculation shows a large deviation from the other two. It seems, therefore, sufficient for the purpose of an approximate estimation of J_{eff} to use 60 beams or so. Figure 7 shows the directional dependence of the profiles of the diagonal total current density obtained by 61 (or 63)-beam calculations. The calculations are performed to obtain $J^{DT}_{<HKL>}$ for three principal zone axes of <100>, <110> and <111>, and for one off-axis direction of incidence ($k_{//} = - g_{2\bar{2}0}$). From these profiles we have estimated the "effective current ratio", J_{eff} for these four directions of incidence. The integrated region S in the numerator of eq. [5] is tentatively taken as a circular region with a radius of 0.1 Å centered at the atomic nucleus. This choice is based on the following simple consideration. Although an atomic displacement can occur only when an electron of 1 MeV is close to the atomic nucleus within the distance of the order of 10^{-4} Å, the target atom is blurred by the thermal vibration to the extent of the order of 0.1 Å. Electrons passing through within the distance of $\sim$ 0.1 Å from the mean position of each atomic nucleus have, therefore, chances to produce knock-ons.

The result of the estimation of the "effective current ratio" for each incident direction is summarized in Table 2. From these calculations it is found that the localization of electrons in the vicinity of the atomic rows is most predominent for the <100> axial case and is reduced by a factor of about two in a slight off-axis direction by about 0.25 degree from the exact <100> axis, ($k_{//} = - g_{2\bar{2}0}$). The values of J_{eff} are also found to decrease in the order of <100>, <111> and <110> from $\sim$ 6 to $\sim$ 4.

3.4 Dependence of incident energies on $J^{DT}_{<100>}$ and J_{eff}

The energy dependence is also examined concerning both the profiles of the diagonal total current density and the "effective current ratio" when the energy of the incident electron is changed from 0.5 to 3 MeV. In this calculation, 61 beams are used for the <100> axial case. The

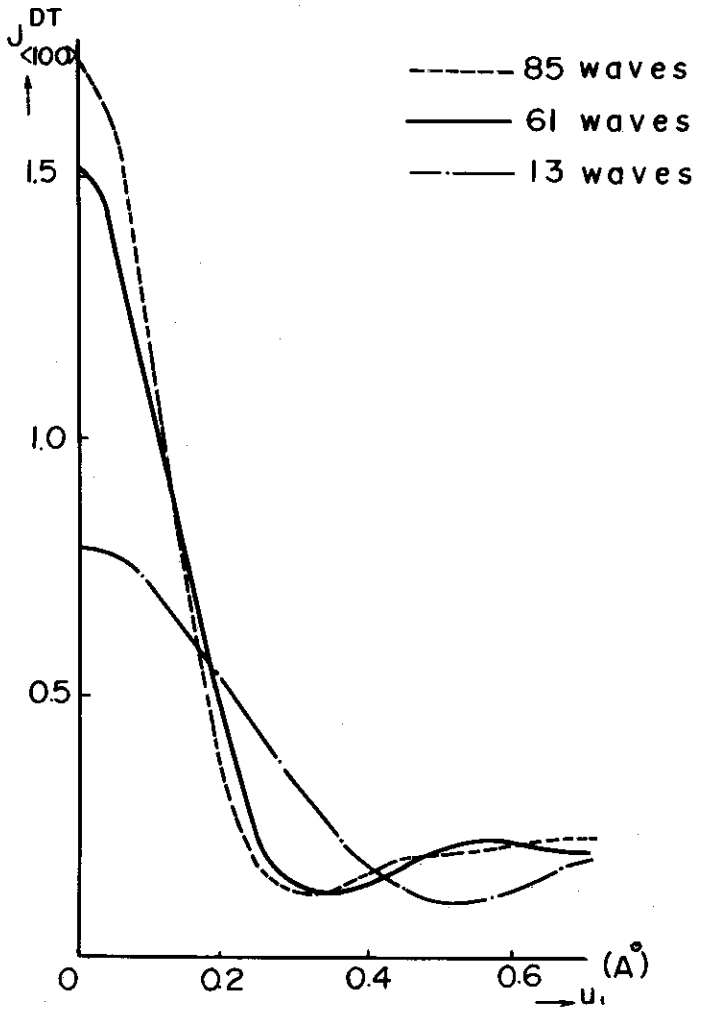

Fig. 6 Effect of the number of beams used for calculating the profiles of the diagonal total current density. The dotted, solid and dash-dotted curves are obtained respectively from 85-, 61-and 13-beam calculations for 1 MeV electrons incident parallel to the <100> axis. The position of an atom is at $u_1 = 0$.

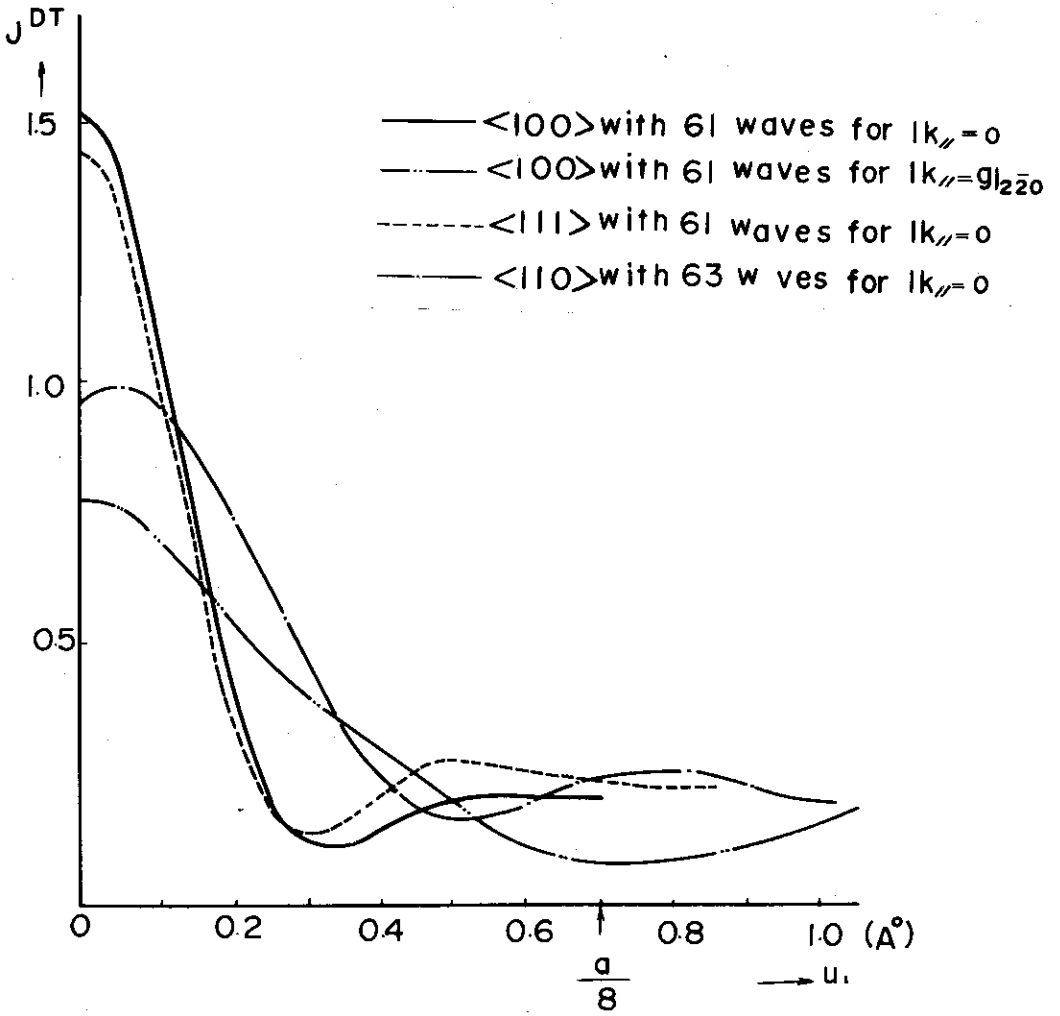

Fig. 7 Directional dependence of the profiles of the diagonal total current density obtained from 61-or 63-beam calculations for the <100>, <111> and <110> axial directions and for the off-axis direction ($k_{//} = - g_{2\bar{2}0}$).

results for the profiles of $J^{DT}_{<100>}$ are showm in Fig. 8. The value of the peak at the position of atomic nucleus is seen to be almost the same for this energy range. The remarkable feature found above ∿ 2 MeV is that the subsidiary maximum occurrs at about 0.4 Å distant from the position of the atomic nucleus, the value of which increases with the energy.

The results of the estimation of the "effective current ratio", J_{eff} are shown in Table 3 for the energies of 0.5, 1, 2 and 3 MeV. Here the same criterion as described in Sec. 3.3 is used for the selection of the integrated area involved in eq. [5]. It is found from this table that the increase of the electron energy results in a slight decrease of the "effective current ratio" for atomic displacement. This is caused by the increase of the current density between the rows of atomic nuclei, typically seen as sub-peaks in Fig. 8. The growth of sub-peaks similar to the above mentioned ones was already found by Kambe et al. in the intensity distribution of Bloch waves excited in a magnesium oxide crystal[5),9)]. They interpreted these sub-peaks as the 2p and 3d type bound states by means of the tight-binding approach to the dynamical theory of electron diffraction. The 2p and 3d type wave fields are the quantized Rosette motions[9)] and therefore considered to have little effect on the damage production.

4. Conclusions

The main purpose of the present calculation is to elucidate the contribution of the locally increased electron current around the rows of atomic nuclei to the damage production due to electrons incident parallel to the principal zone axis. The distribution of the electron current density in a germanium crystal is investigated in detail by using the many-beam theory of electron diffraction without absorption. The main results of the calculation are summarized in the following:

(1) The distribution of the total current density in the transverse plane is found to oscillate periodically with depth. That is, in the axial case a highly localized distribution and a nearly flat distribution of current density in the transverse plane appear alternatively with a definite period of the depth. This period may be called as "localization period of electron current". For example, the period is found to be ∿ 190 Å for 1 MeV electron in the <100> axial case from the 61-beam calculation. In the slightly off-axis case the

results for the profiles of $J^{DT}_{<100>}$ are showm in Fig. 8. The value of the peak at the position of atomic nucleus is seen to be almost the same for this energy range. The remarkable feature found above ∿ 2 MeV is that the subsidiary maximum occurrs at about 0.4 Å distant from the position of the atomic nucleus, the value of which increases with the energy.

The results of the estimation of the "effective current ratio", J_{eff} are shown in Table 3 for the energies of 0.5, 1, 2 and 3 MeV. Here the same criterion as described in Sec. 3.3 is used for the selection of the integrated area involved in eq. [5]. It is found from this table that the increase of the electron energy results in a slight decrease of the "effective current ratio" for atomic displacement. This is caused by the increase of the current density between the rows of atomic nuclei, typically seen as sub-peaks in Fig. 8. The growth of sub-peaks similar to the above mentioned ones was already found by Kambe et al. in the intensity distribution of Bloch waves excited in a magnesium oxide crystal[5),9)]. They interpreted these sub-peaks as the 2p and 3d type bound states by means of the tight-binding approach to the dynamical theory of electron diffraction. The 2p and 3d type wave fields are the quantized Rosette motions[9)] and therefore considered to have little effect on the damage production.

4. Conclusions

The main purpose of the present calculation is to elucidate the contribution of the locally increased electron current around the rows of atomic nuclei to the damage production due to electrons incident parallel to the principal zone axis. The distribution of the electron current density in a germanium crystal is investigated in detail by using the many-beam theory of electron diffraction without absorption. The main results of the calculation are summarized in the following:

(1) The distribution of the total current density in the transverse plane is found to oscillate periodically with depth. That is, in the axial case a highly localized distribution and a nearly flat distribution of current density in the transverse plane appear alternatively with a definite period of the depth. This period may be called as "localization period of electron current". For example, the period is found to be ∿ 190 Å for 1 MeV electron in the <100> axial case from the 61-beam calculation. In the slightly off-axis case the

Table 2 Directional dependence of the value of the "effective current ratio", J_{eff}

Direction	<100> $k_{//}=0$	<100> $k_{//}=-g_{2\bar{2}0}$	<111> $k_{//}=0$	<110> $k_{//}=0$
J_{eff}	6.1	3.3	5.3	4.3

Table 3 Energy dependence of the "effective current ratio", J_{eff}

Energy (MeV)	3.0	2.0	1.0	0.5
J_{eff}	5.3	5.6	6.0	7.2

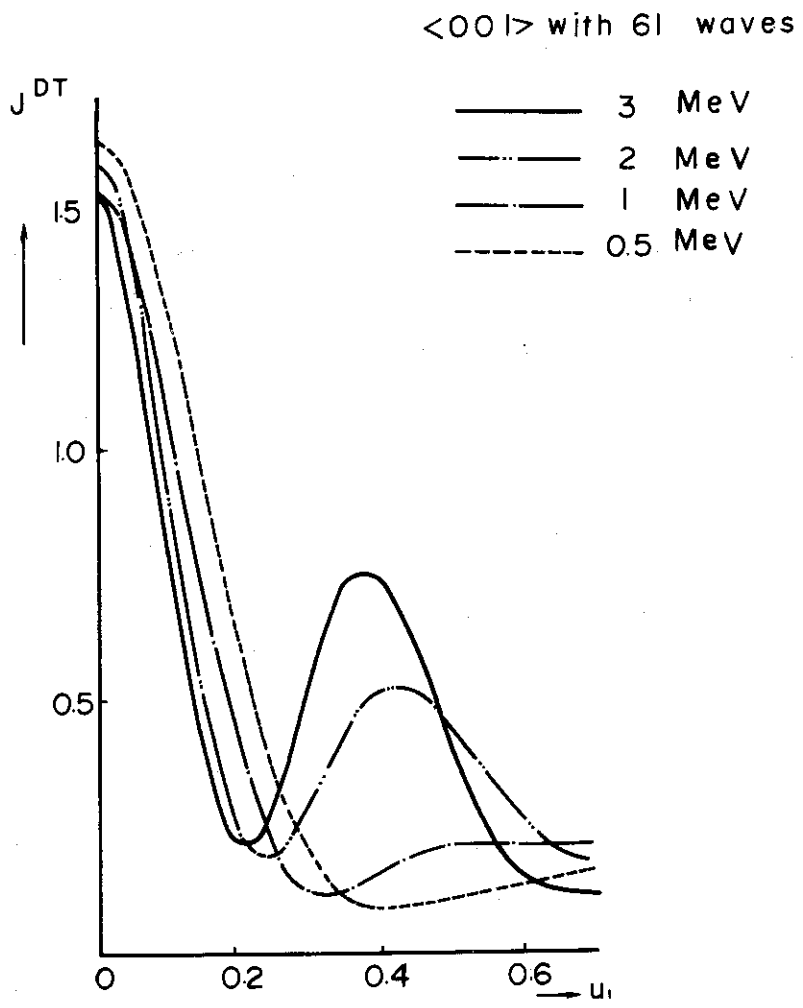

Fig. 8 The variation of the profiles of the diagonal total current density with the increase of the energy from 0.5 MeV to 3 MeV for the <100> axial case obtained by 61-beam calculation. The characteristic sub-peak occurs at about 0.4 Å distant from the position of an atomic nucleus above ∿ 2 MeV.

period becomes somewhat irregular.

(2) The two-dimensional, transverse distribution of the diagonal total current densities which are the depth averages of the total ones are examined for the <100>, <110>, <111> and <120> axial cases, respectively. The "effective current ratio" for atomic displacement is defined as a ratio of the localized diagonal current density at the atomic position to the mean current density. This quantity is estimated for 1 MeV electrons to be about 6, 5 and 4 for the <100>, <111> and <110> axial cases, respectively.

(3) The energy dependence of the localization of the diagonal total current density is examined and found that the effective current ratios decrease slightly with increasing the energy of incident electrons.

Acknowledgements

The authors wish to express their hearty thanks to Dr. K. Sasaki for his helpful discussion and one of them (T.N.) to Dr. T. Asaoka for his continued interests and encouragement.

References

1) For review, Jung P.: Atomic Collision in Solids, edited by S. Datz et al., 87 (Plenum Press, 1975)
2) For review, Channeling, edited by D. V. Morgan (Jhon Wiley & Sons, London, 1973)
3) Howie A.: Phil. Mag., 14, 223 (1966)
4) Lehmpfull G.: Z. Naturforsh., 28a, 1 (1973)
5) Kambe K., Lehmpfull G. and Fujimoto F.: Z. Naturforsh., 29a, 1034 (1974)
6) Hashimoto H., Endoh H. and Kumao A.: Proc. 4th Int. National Conf. HVEM (Toulouse) (1975)
7) Nishida T. and Izui K.: JAERI-M 5441 in Japanese (1973)
8) Smith G.H. and Burge R.E.: Acta Cryst., 15, 182 (1962)
9) Fujimoto F., Komaki K., Fujita H., Sumita N., Uchida Y., Kambe K. and Lehmpfuhl G.: Atomic Collision in Solids 2, edited by S. Datz et al., 547 (Plenum Press, 1975)